Plant Cell Physiol. 45(5): 503–510 (2004)

Rapid Paper

Loss of Plastidic Lysophosphatidic Acid Acyltransferase Causes Embryo-Lethality in *Arabidopsis*

Bin Yu, Setsuko Wakao, Jilian Fan and Christoph Benning [1]

Department of Biochemistry and Molecular Biology, Michigan State University, East Lansing, MI 48824-1319, U.S.A.

Phosphatidic acid is a key intermediate for chloroplast membrane lipid biosynthesis. De novo phosphatidic acid biosynthesis in plants occurs in two steps: first the acylation of the *sn*-1 position of glycerol-3-phosphate giving rise to lysophosphatidic acid; second, the acylation of the *sn*-2 position of lysophosphatidic acid to form phosphatidic acid. The second step is catalyzed by a lysophosphatidic acid acyltransferase (LPAAT). Here we describe the identification of the *ATS2* gene of *Arabidopsis* encoding the plastidic isoform of this enzyme. Introduction of the *ATS2* cDNA into *E. coli* JC 201, which is temperature-sensitive and carries a mutation in its LPAAT gene *plsC*, restored this mutant to nearly wild type growth at high temperature. A green-fluorescent protein fusion with ATS2 localized to the chloroplast. Disruption of the *ATS2* gene of *Arabidopsis* by T-DNA insertion caused embryo lethality. The development of the embryos was arrested at the globular stage concomitant with a transient increase in *ATS2* gene expression. Apparently, plastidic LPAAT is essential for embryo development in *Arabidopsis* during the transition from the globular to the heart stage when chloroplasts begin to form.

Keywords: Embryo development — Fatty acid biosynthesis — Lipid metabolism — Lipid trafficking — Plastid pathway — Thylakoid membrane.

Abbreviations: ACP, acyl carrier protein; DAG, diacylglycerol; ER, endoplasmic reticulum; G3P, glycerol-3-phosphate; GFP, green fluorescent protein; LPA, lysophosphatidic acid; LPAAT, lysophosphatidic acid acyltransferase; MGDG, monogalactosyldiacylglycerol; PA, phosphatidic acid; PG, phosphatidylglycerol.

Introduction

The thylakoid membrane of photosynthetic organisms contains four major glycerolipids, mono- and digalactosyldiacylglycerol, phosphatidylglycerol (PG), and the sulfolipid sulfoquinovosyldiacylglycerol. Two pathways contribute to the biosynthesis of membrane lipids in many plants including *Arabidopsis* (Roughan and Slack 1982). According to this "two pathway hypothesis", fatty acids synthesized de novo in the chloroplast and bound to the acyl carrier protein (acyl-ACP) are either directly incorporated into glycerolipids in the chloroplast envelopes or are exported to the endoplasmic reticulum (ER). At the ER, they serve in the form of acyl-CoAs as precursors for extraplastidic glycerolipids. A fraction of the diacylglycerol moieties derived from phosphatidylcholine is returned to the chloroplast and enters thylakoid lipid biosynthesis. As a consequence, diacylglycerol (DAG) moieties of plastidic and extra-plastidic origin are found in the glycerolipids of the thylakoid membranes of *Arabidopsis*.

A critical intermediate of both pathways in plants is phosphatidic acid (PA), which is also essential for the biosynthesis of glycerolipids and triacylglycerols in bacteria, yeast and animals. A deficiency for PA biosynthesis is lethal in *Escherichia coli* consistent with an essential role for PA in this bacterium (Coleman 1990). Unlike animals and yeast, in plants the glycerol-3-phosphate (G3P) pathway is thought to be the only pathway for the de novo PA biosynthesis (Athenstaedt and Daum 1999). Two acylations are involved: first the transfer of an acyl group from either acyl-ACP or acyl-CoA to the *sn*-1 position of G3P catalyzed by a G3P acyltransferase leading to the formation of 1-acyl-*sn*-G3P (lysophosphatidic acid, LPA). This intermediate is further acylated to PA by an 1-acyl-*sn*-G3P acyltransferase (LPAAT). In plants, LPAAT activity is associated with multiple membrane systems, including chloroplasts, ER, and the outer membrane of mitochondria, suggesting the presence of several different isoforms.

Genes encoding the G3P acyltransferase have been isolated from different plant species (Bhella and Mackenzie 1994, Ishizaki-Nishizawa et al. 1995, Ishizaki et al. 1988, Nishida et al. 1993, Weber et al. 1991). Generally, the *sn*-1 position of PA typically contains 16 or 18 carbons indicating that this enzyme does not discriminate between these two fatty acid substrate classes. However, in some plant species, G3P acyltransferase seems to be more specific. For instance, in *Arabidopsis*, the ATS1 (ACT1) protein, the plastidic isoform of G-3-P acyltransferase, has considerable substrate preference for 18-carbon fatty acids (Yokoi et al. 1998). Of the enzymes acting on LPA, the plastidic LPAAT prefers 16-carbon fatty acids and the ER form 18-carbon fatty acids. This substrate specificity provides the means to distinguish thylakoid lipid species derived from

[1] Corresponding author: E-mail, benning@msu.edu; Fax, +1-517-353-9334.

the plastid or ER-pathways based on the fatty acids at the *sn*-2 position. Furthermore, the distinct substrate specificities of the different LPAAT isoforms are a critical factor in determining the overall lipid acyl composition in plants. To date, several cDNAs encoding plant LPAATs have been isolated from coconut (Davies et al. 1995, Knutzon et al. 1995), the immature embryo of meadow foam (Brown et al. 1995, Hanke et al. 1995), the maize endosperm (Brown et al. 1994) and from *Brassica napus* (Bourgis et al. 1999). Among these enzymes, BAT2 of *B. napus* has been shown to be a plastid-localized isoform. However, the in vivo roles for this enzyme are still unknown due to the lack of lines with altered activity. In *Arabidopsis*, inactivation of the plastidic G3P acyltransferase in the *ats1* (*act1*) mutant led to the loss of the plastid pathway for glycolipid biosynthesis (Kunst et al. 1988). A surprising observation was that despite the drastic effects on plastidic glycolipid biosynthesis, PG biosynthesis was only mildly impaired in the *ats1* (*act1*) mutant. However, it is not clear whether the currently described alleles for *ats1* (*act1*) are leaky, a caveat that makes it difficult to draw definitive conclusions regarding the function of the enzyme and leaves the interpretation of the mutant phenotype ambiguous. This study was conducted to gain a better understanding of the origin of PA in plants and to determine the in vivo function of plastidic LPAAT. As will be described in detail, the respective null-mutant leads to embryolethality, an unequivocal demonstration of the essential function of plastidic LPAAT in *Arabidopsis*.

Results

Identification of an Arabidopsis ATS2 candidate gene

Taking advantage of the published *Arabidopsis* genome, we identified an *Arabidopsis* gene At4g30580 (GenBank accession no. NP_194787) on chromosome 4 as a putative ortholog of *BAT2* from *B. napus*. A wild-type cDNA corresponding to gene At4g30580 was isolated by reverse transcription-PCR and sequenced. This cDNA encoded 356 amino acids in agreement with the protein predicted from the genomic sequence. The protein was designated ATS2 following the gene designation at TAIR (www.Arabidopsis.org) for the plastidic G3P acyltransferase in *Arabidopsis*, ATS1 (ACT1). Using the BLAST2 sequence alignment software (Altschul et al. 1997), it showed 80% identity, and 85% similarity over 344 amino acid residues with BAT2 (Fig. 1A). Like for BAT2, three putative membrane-spanning domains were predicted for ATS2 by the TMHMM software (Sonnhammer et al. 1998).

To explore the evolutionary origin of LPAATs, we performed a phylogenetic analysis with ATS2 and other putative and bona fide LPAATs. The experimentally verified LPAATs included enzymes from *E. coli* (Coleman 1992), human (AGPAT1, AGPAT2) (Eberhardt et al. 1997, West et al. 1997), *Limnanthes douglasii* (LAT1, LAT2) (Brown et al. 1995) and *L. alba* (meadow foam) (Lassner et al. 1995), coconut

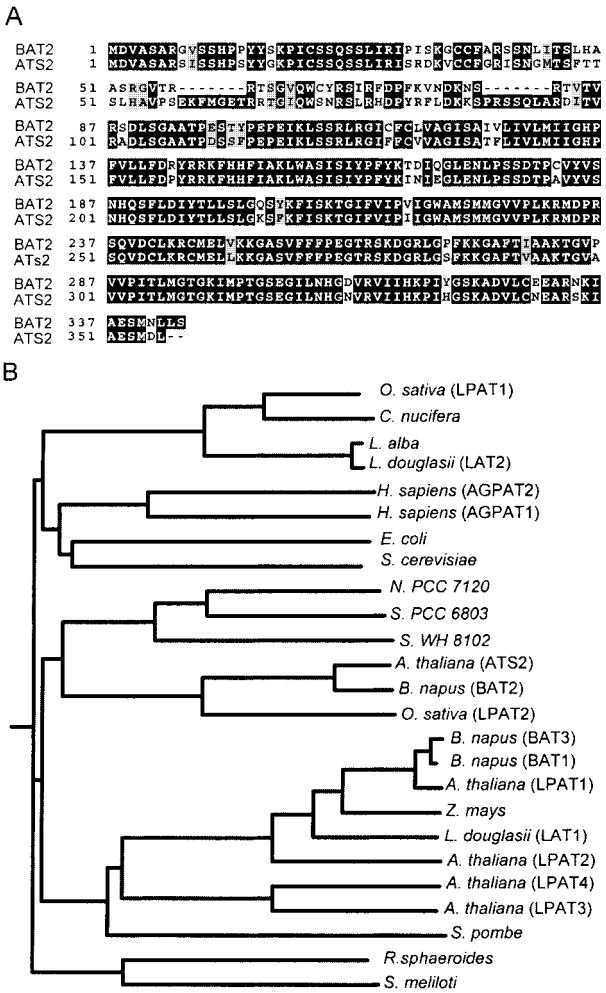

Fig. 1 Evolutionary relationship between LPAATs. Sequence alignment of BAT2 and ATS2 (A). Identical amino acids are indicated by black boxes, similar ones are shaded grey. (B) Phylogenetic relationship of LPAATs. The following proteins were included in the analysis (GenBank accession no.): *Arabidopsis thaliana ATS2* (NP_194787); *A. thaliana* LPAT1 (NP_567052); *A. thaliana* LPAT2 (NP_175537); *A. thaliana* LPAT3 (NP_565098); *A. thaliana* LPAT4 (NP_188515); *Brassica napus* BAT1 (CAA90019); *B. napus* BAT2(AF111161); *B. napus* BAT3 (CAB09138); *Oryza sativa* LPAT1 (CAE03516); *O. sativa* LPAT2 (AAL58271); *Limnanthes alba* (Q42868); *Limnanthes douglasii* LAT2 (CAA86877); *L. douglasii* LAT1 (CAA88620); *Cocos nucifera* (Q42670); *Synechococcus sp.* WH 8102 (NP_898339); *Nostoc* sp. PCC 7120 (NP_484285); *Synechocystis* sp. PCC 6803 (NP_441924); *Saccharomyces cerevisiae* (NP_010231); *Schizosaccharomyces pombe* (NP_595192); *Escherichia coli* (NP_417490); *Homo sapiens* AGPAT1 (AAH03007); *H. sapiens* AGPAT2 (AAH07269); *Sinorhizobium meliloti* (NP_386764); *Rhodobacter sphaeroides* (ZP_00008109).

(Knutzon et al. 1995), *B. napus* (BAT1 and BAT2) (Bourgis et al. 1999), yeast (Nagiec et al. 1993), and maize (Brown et al. 1994). Predicted LPAATs were those from *A. thaliana* (LPAT1-4), *Oryza sativa* (LPAT1-2), *B. napus* (BAT3), *Schizosaccharomyces pombe*, the bacteria *Rhodobacter sphaeroides* and *Sinorhizobium meliloti* and different cyanobacteria as indicated.

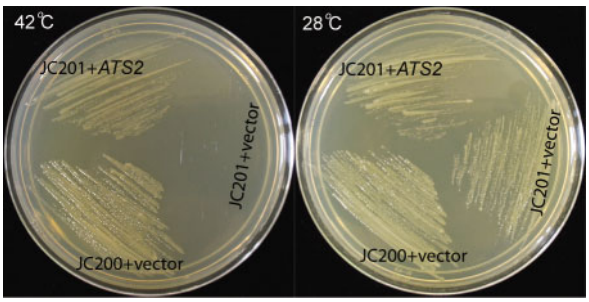

Fig. 2 Heterologous complementation of *E. coli* JC201 by expression of *ATS2* of *Arabidopsis*. Strain JC200 is the *E. coli* wild-type *plsC* control strain isogenic to JC201.

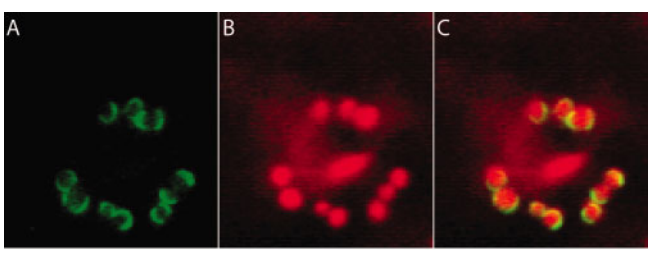

Fig. 3 Subcellular localization of the ATS2 protein. (A) ATS2-GFP fusion protein, (B) chlorophyll fluorescence, (C) overlay of (A) and (B).

Of these LPAATs, LPAT2 from *O. sativa* is a putative plastidic isoform based on the predicted presence of a chloroplast transit peptide. Fig. 1B shows a phylogenetic tree derived from protein sequence alignments. The ATS2 protein clustered with two plastidic LPAATs on a branch alongside the cyanobacterial cluster. ATS2 appears to represent a highly conserved plastidic LPAAT. It shared 68% and 91% identity, respectively, with *O. sativa* and *B. napus* over 207 amino acids representing the domain aligning with the bacterial sequence encoded by *plsC*.

Expression of the ATS2 cDNA complements an E. coli LPAAT mutant

To demonstrate directly that *ATS2* encodes an LPAAT, we tested if the expression of the *ATS2* cDNA rescued the temperature-sensitive phenotype of *E. coli* strain JC201. This strain is unable to grow at 42°C but grows well at 30°C due to the deficiency of LPAAT activity (Coleman 1990). Thus, the test is based on the restoration of its growth at the non-permissive temperature. This strategy was successfully used to isolate LPAATs from many other organisms (Brown et al. 1994, Davies et al. 1995, Eberhardt et al. 1997, West et al. 1997, Bourgis et al. 1999). A truncated version of the *ATS2* cDNA lacking the sequence encoding the putative chloroplast transit peptide was fused to the *lacZ* gene which was under the control of an inducible promoter. The result shown in Fig. 2 indicates that the vector expressing *ATS2*, but not the empty vector rescued the temperature sensitivity of *E. coli* JC201. This result suggested that *ATS2* of *Arabidopsis* indeed encodes an LPAAT that can substitute for the inactive bacterial LPAAT in the mutant.

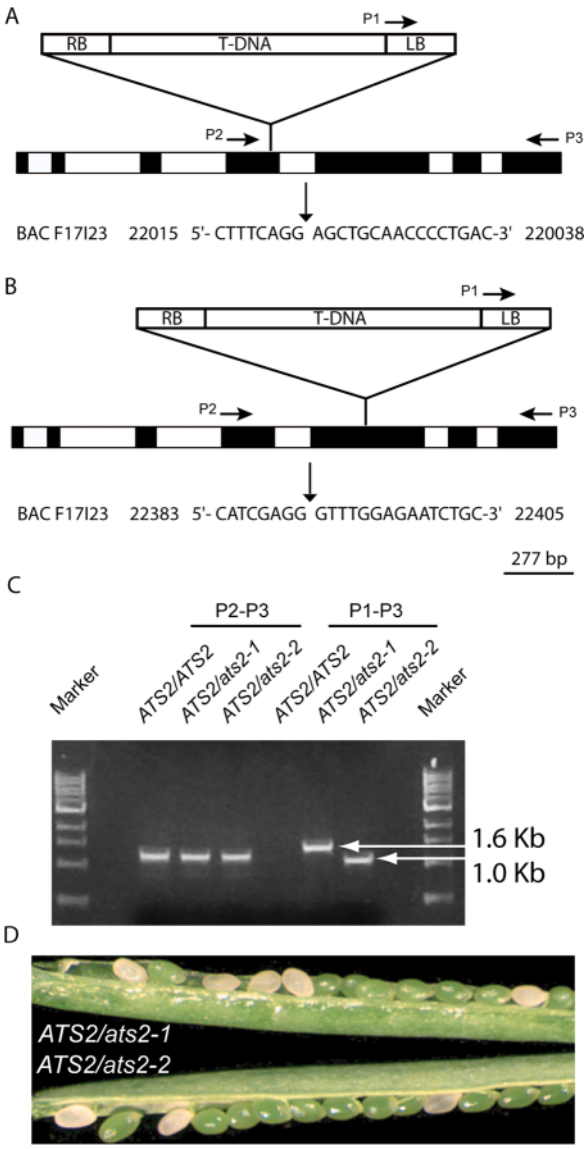

Fig. 4 Isolation and characterization of *ATS2* T-DNA insertion lines. (A) Insertion into the *ATS2* gene in the heterozygous *ATS2-1/ats2-1* allele and (B) into the *ATS2-2/ats2-2* allele. Black boxes represent exons, open boxes introns. The exact insertion site (based on the sequence of BAC F17I23 GenBank accession no. AF160182) is indicated by a vertical arrow. Horizontal arrows labeled P1, P2, P3 represent the binding site locations for PCR primers. (C) PCR results for genomic DNA isolated from the wild type (*ATS2/ATS2*) and the two allelic heterozygous mutant lines (*ATS2-1/ats2-1* and *ATS2-2/ats2-2*). The primer combination P2-P3 is diagnostic for the endogenous gene, the combination P1-P3 for the T-DNA flanking genomic DNA as indicated in (A) and (B). (D) Dissected green siliques of heterozygous mutant lines (alleles as indicated) showing the segregation of clear white seeds.

Localization of the ATS2 protein

The ATS2 protein sequence has a predicted 56 amino acid N-terminal chloroplast transit peptide (ChloroP) (Emanuelsson et al. 1999). To experimentally verify the subcellular localiza-

Table 1 Segregation and complementation analysis of the two allelic heterozygous *ATS2/ats2* lines

	Green seeds	White seeds	χ^2 (P <0.1)
ATS2-1/ats2-1	413	135	0.04 (3 : 1)
ATS2-2/ats2-2	353	120	0.03 (3 : 1)
ATS2-1/ats2-1 (*ATS2 cDNA*)	498	35	0.09 (15 : 1)
ATS2-2/ats2-2 (*ATS2 cDNA*)	540	38	0.10 (15 : 1)

Multiple siliques from single plants were analyzed. The heterozygous state of *ATS2/ats2* was confirmed by genotyping using PCR (cf. Fig. 4C).

tion of ATS2, the *ATS2* cDNA was fused to the N-terminus of the green fluorescent protein (GFP) cDNA. The resulting construct was expressed in transgenic wild-type plants under the control of the 35S cauliflower mosaic virus (CMV) promoter. The GFP fluorescence in transgenic plants was observed using confocal microscopy. As shown in Fig. 3, the GFP fluorescence was exclusively associated with chloroplasts. In control plants expressing only the GFP cDNA, green fluorescence was not associated with chloroplasts but appeared to be diffuse in the cell. Based on these results, it was concluded that ATS2 is localized in the plastid. These results were also consistent with findings of proteomics studies detecting the presence of this protein in chloroplast preparations (Ferro et al. 2002, Ferro et al. 2003).

Isolation of mutants with T-DNA insertion into ATS2

In an attempt to investigate the function of ATS2 in the chloroplast, two T-DNA insertion lines, SALK_073445 and SALK_108812, (alleles *ats2-1* and *ats2-2* respectively) were identified in the Salk T-DNA insertion population (Alonso et al. 2003). The T-DNA insertion sites were determined by sequencing PCR products obtained with a combination of gene- and T-DNA-specific primers as shown in Fig. 4. The *ats2-1* allele carried a T-DNA insertion in the fourth exon of the predicted At4g30580 gene (Fig. 4A) at base pair 22,022 of the sequence of BAC F17I23 (GenBank accession no. AF160182) and the *ats2-2* allele in the fifth exon at base pair 22,390 (Fig. 4B). Despite extensive screening, no homozygous plants could be identified. Combinations of gene-specific and T-DNA-specific primers to generate PCR products diagnostic for mutant and wild-type chromosomes and a typical result for wild-type and *ATS2/ats2-1* and *ATS2/ats2-2* heterozygous lines are shown in Fig. 4C. Both mutant lines showed insert-specific as well as wild-type genomic DNA fragments. Furthermore, when immature siliques were opened which grew on heterozygous plants as confirmed by genotyping, approximately 25% of the seeds were clear white (Fig. 4D), indicative for the arrest of embryo development at an early stage. This observation raised the possibility that a homozygous *ats2* null-mutant was embryo-lethal. To quantify this phenomenon, one or two siliques from 10 heterozygous plants were opened and the ratio of viable to aborted

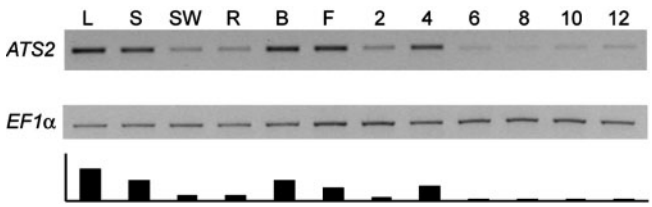

Fig. 5 Expression of *ATS2* in various tissues and during silique development. Semi-quantitative RT-PCR was used and products for *ATS2* are shown in comparison to the control gene *EF1α* (GenBank accession no. NM_125432). Relative levels of *ATS2* normalized to *EF1α* are shown in the bottom panel. Lanes from left to right: L, leaf; S, stem; SW, silique wall (age 5 d after flowering); R, root; B, bud; F, flower; 2–12, siliques of different development stages as indicated (days after flowering).

seeds in all the siliques examined was obtained as shown in Table 1. These data were consistent with a 3 : 1 segregation ratio as expected for a recessive mutation in an essential nuclear gene. When viable plants derived from *ATS2/ats2-1* heterozygous lines or *ATS2/ats2-2* were analyzed, approximately two thirds (39 out of 61 for *ATS2/ats2-1* and 42 out of 62 for *ATS2/ats2-2*) produced aborted seeds consistent with a 2-to-1 ratio of heterozygous to wild-type genotypes among the surviving plants.

Complementation of the embryo-lethal phenotype was tested by introduction of the wild-type *ATS2* cDNA under the control of the 35S-CMV promoter into *ATS2/ats2* heterozygous plants. In the T1 generation, transgenic plants were selected on hygromycin B containing medium and tested for GFP expression. Three classes were expected among the transgenic plants: homozygous mutants (*ats2/ats2*), heterozygous plants (*ATS2/ats2*) and homozygous wild-type plants (*ATS2/ATS2*). Because a single copy of the transgene would behave like a second (dominant) genetic marker in this experiment, complementation would be in effect if homozygous mutant lines segregated 1/4 white seeds, heterozygous lines 1/16 white seeds, and homozygous wild-type lines no white seeds. All three classes were observed among 10 transgenic plants tested, indicating complementation. Because transgenic heterozygous plants were most informative, one plant for each allele was analyzed in detail. Genotyping by PCR (cf. Fig. 4C) confirmed these plants to be *ATS2/ats2* heterozygous and analysis of seeds in immature siliques indicated the presence of 1/16 white seeds (Table 1) as expected for complementation.

Because of the embryo lethality, no further phenotypic analysis was feasible on homozygous lines. When heterozygous lines were analyzed, no changes in growth or leaf fatty acid composition were observed (data not shown).

A transient increase in ATS2 expression in developing siliques in the wild type corresponds to the arrest of embryo development in the mutant

Analyzing the expression of the *ATS2* gene, the mRNA was detected in all tissues tested (Fig. 5), as would be expected

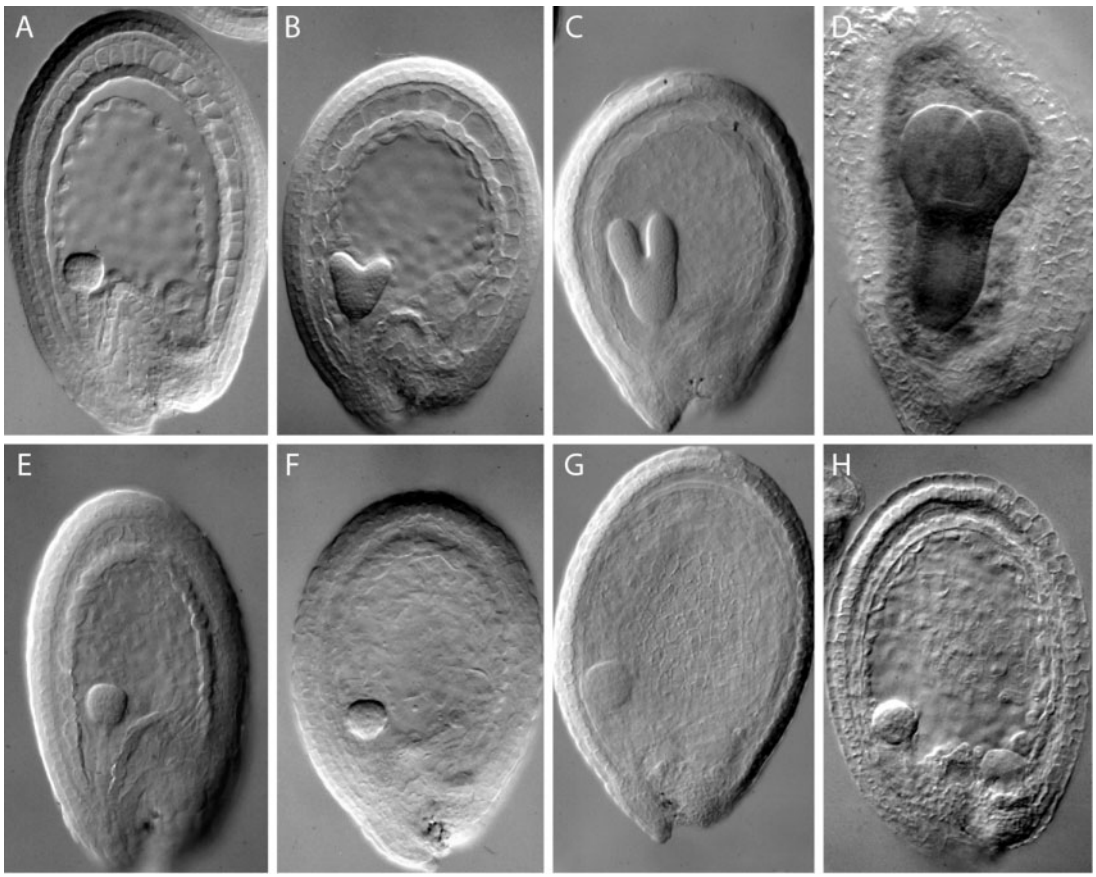

Fig. 6 Arrest of embryo development. Four siliques of different developmental age growing on heterozygous *ATS2/ats2-1-1* plants were dissected. (A, E), two representative embryos from the youngest silique, in which all embryos were at the globular stage and indistinguishable; (B, F), older silique with most embryos at the heart stage (B) and with about 25% of the embryos arrested at the globular stage (F); (C) developing early torpedo stage embryo and (G) arrested embryo from the same silique at the globular stage; (D), oldest silique with developing embryo at the late torpedo stage and (H) globular arrested embryo from the same silique.

for a gene involved in an essential process. Interestingly, *ATS2* mRNA abundance was reduced in silique walls compared to leaves and the abundance was higher in RNA samples from intact siliques. This result suggested an increased expression of *ATS2* in developing seeds. Because it is exceedingly difficult to obtain sufficient amounts of mRNA from very young embryos, a time course of developing intact siliques was analyzed. Comparison to the silique wall sample (5 d after flowering) should provide an indication of mRNA abundance in the developing seed. Interestingly, *ATS2* expression transiently increased in siliques 4 d after flowering (Fig. 5).

Embryo development was compared by Nomarski microscopy in different developing seeds of siliques growing on heterozygous plants (Fig. 6). Before the onset of visible chlorophyll accumulation at the transition from globular to the early heart stage (Mansfield et al. 1991), the embryos were indistinguishable. However, in older siliques, seeds with arrested development became visible to the naked eye and closer examination revealed that the clear white seeds contained embryos arrested at the globular stage. Presumably, these seeds corresponded to dark brown aborted seeds apparent in mature siliques. It should be noted that the transient increase in *ATS2* expression observed for the wild type 4 d after flowering (Fig. 5) corresponded to the transition in embryo development from the globular to the heart stage, when the developmental arrest occurs in a quarter of the seeds developing in siliques on heterozygous plants.

Discussion

With the availability of the *Arabidopsis* genome sequence (The Arabidopsis Genome Initiative 2001) it has become feasible to predict genes encoding enzymes involved in lipid metabolism in *Arabidopsis* based on sequence similarity to enzymes with known functions from bacteria and other plants. Ohlrogge and coworkers have used this approach to assemble a catalog of lipid metabolism genes in *Arabidopsis* (Beisson et al. 2003). As we now know based on the present study, they correctly annotated *Arabidopsis* gene At4g30580 to encode a plastidic LPAAT. Functional proof was provided by heterologous com-

plementation of the *E. coli* LPAAT-deficient *plsC* mutant (Fig. 2). Furthermore, subcellular localization of the ATS2-GFP fusion (Fig. 3) agreed with a plastidic localization of the protein as predicted. Independent experimental evidence for a plastid localization of ATS2 was also obtained by Ferro and colleagues (Ferro et al. 2002, Ferro et al. 2003). When confirmed and putative LPAAT protein sequences from different organisms were aligned and grouped based on the amino acid sequence similarity, ATS2 of *Arabidopsis* clustered with BAT2 from *B. napus* and LPAT2 from *O. sativa*, both plastidic LPAATs (Fig. 3). Furthermore, these plastidic LPAATs formed a subcluster with cyanobacterial LPAATs providing supportive evidence for the cyanobacterial endosymbiont origin of chloroplasts. Four other putative *Arabidopsis* LPAATs were grouped in a distinct cluster representing microsomal LPAATs (Fig. 1) suggesting that their evolutionary origin is different from that of plastidic isoforms. One of the most versatile resources to shed light on the function of a particular gene in *Arabidopsis* is the broad availability of sequenced T-DNA insertion lines (Alonso et al. 2003). In the case of *ATS2*, two independent alleles were available, both of which gave rise to a striking phenotype, embryo-lethality. The presence of two independent alleles and restoration of embryo development following the transgenic expression of the *ATS2* cDNA (genetic complementation) linked the embryo defect to the T-DNA inactivation of the gene encoding plastidic LPAAT in the two allelic mutants. The result was surprising, because a mutant in the plastidic G3P acyltransferase gene, *ATS1* (*ACT1*), affecting the step prior to ATS2 in the pathway, had no effect on embryo development, despite the fact that the plastid pathway of thylakoid lipid biosynthesis was strongly impaired in this mutant (Kunst et al. 1988). However, it should be noted that it is not clear at this time to which extent the *ats1* (*act1*) mutant is "leaky", if at all, because plastidic PG, which is assumed to be synthesized by the plastid pathway of membrane lipid biosynthesis, was only moderately reduced in the mutant. The complete loss of PG in the *ats2* mutants could not be the cause for the observed embryo arrest, because homozygous null-alleles of the *PGP1* gene encoding plastidic phosphatidylglycerolphosphate synthase gave rise to seedlings lacking plastidic PG (Hagio et al. 2002, Babiychuk et al. 2003). However, these mutant seedlings were completely white and non-photosynthetic. Therefore, either the absence of plastidic PA as a critical intermediate or signaling molecule, or the accumulation of lyso-PA harmful to membrane integrity might be the cause of the observed embryo lethality in the *ats2* mutants. The fact that embryo development was arrested just at the transition from the globular to the heart stage, when thylakoid membranes start to develop and a corresponding peak in *ATS2* gene expression was observed (Fig. 5), suggests that the lack of PA, which also has a regulatory function (Meijer and Munnik 2003), might be the main cause of embryo arrest in the *ats2* mutants. However, other possibilities cannot be ruled out at this time. While embryo-lethality is an easily observable phenotype, the respective null-mutants provide no detailed information on the role of plastidic ATS2, because homozygous lines could not be further analyzed and heterozygous lines lacked any phenotype. Mutations with leaky alleles in *ATS2* giving rise to viable plants with milder phenotypes will have to be isolated and studied to better understand the role of PA in plant metabolism.

Materials and Methods

Plant materials and growth

Surface-sterilized seeds were germinated on 0.8% (w/v) agar-solidified Murashige and Skoog (MS) medium (Murashige and Skoog 1962) containing 1% sucrose. Seedlings (10 d old) of *Arabidopsis* wild type and mutants were transferred to soil drenched with half-strength *Arabidopsis* nutrient solution (Estelle and Somerville 1987), and grown under a photosynthetic photon flux density of 70–80 mol m^{-2} s^{-1} at 22/18°C (day/night) with a 14-h light/10-h dark period.

Bioinformatics

For routine sequence comparison, BLAST2 was used (Altschul et al. 1997). Multiple sequence alignment was done by CLUSTAL W software (Thompson et al. 1994) at The Biology Work Bench (http://workbench.sdsc.edu/). Prediction of chloroplast transit peptides was accomplished using ChloroP (Emanuelsson et al. 1999). Transmembrane spanning helices were predicted using TMHMM (Sonnhammer et al. 1998).

T-DNA insertion analysis, ATS2 cDNA cloning and expression in transgenic plants

The T-DNA insertional mutants, *ats2-1* (SALK_073445) and *ats2-2* (SALK_108812) were obtained from the Arabidopsis Stock Center (www.arabidopsis.org). The T-DNA left border primer P1 5′-GTTCACGTAGTGGGCCATCG-3′, and gene-specific primers P2 5′-CAGGTACCTTAGAGATCCATTGATTCTGC-3′ and P3 5′-GAGGATCCAGTGAAAAATTTATGGGCGA-3′ were used to screen the plants for T-DNA insertions (cf. Fig. 4). The T-DNA-bordering DNA fragments were ligated into the plasmid pPCR-script AMP SK(+) (Stratagene, La Jolla, CA, U.S.A.), and sequenced to determine the localization of the T-DNA insertion. The *ATS2* open reading frame corresponding to *Arabidopsis* gene At4g30580 (GenBank accession no. NP_194787) was predicted from the DNA sequence of BAC F17I23_80 (GenBank accession no. AF160182) and amplified by reverse transcription-PCR using the primers 5′-GAGGATCCATGGATGTCGCTTCTGCTCG-3′ and 5′-CAGGTACCTTAGAGATCCATTGATTCTGC-3′. For this purpose, total leaf RNA was isolated from 20-day-old plants (Col-2) according to the method by Logemann et al. (1987). Reverse transcription-PCR was performed by using the ProSTAR HF system from Stratagene (La Jolla, CA, U.S.A.). The PCR product was inserted into the ligation-ready Stratagene vector pPCR-Script Amp SK(+) giving rise to pATS2. For plant transformation, the insert of pATS2 containing the full-length coding sequence of *ATS2* including the transit peptide was amplified by PCR using the primers 5′-GGACTAGTGATGTCGCTTCTGCTCGGA-3′ and 5′-GGACTAGTGAGATCCATTGATTCTGCA-3′. This fragment was inserted into the binary vector pCAMBIA1304 (www.cambia.org) using the *Spe*I restriction site to give plasmid pCATS2. Based on the nature of pCAMBIA1304, this construct led to the expression of an ATS2-GFP (green fluorescent protein) fusion protein and the resulting plants were used in the complementation and localization analysis. Stable transformation of *Arabidopsis* was achieved using the vacuum infiltration method (Bechtold and Pelletier 1998). Transgenic plants were select-

ed in the presence of hygromycin B (25 μg ml^{-1}) on MS medium lacking sucrose.

Semi-quantitative RT-PCR

Total RNA was extracted from plant tissues other than developing siliques with an RNA extraction kit (RNeasy, QIAGEN, Valencia, CA, U.S.A.). Silique RNA was extracted from frozen tissue (50–100 mg) which was ground in 1.5-ml tubes. To the powder 350 μl of pre-heated (80°C) extraction buffer (0.02 M sodium borate, 30 mM EDTA, 30 mM EGTA, 1% sodium dodecylsulfate, 2% deoxycholate, 2% polyvinylpolypyrrolidone, 2% polyvinylpyrrolidone 40K, 100 mM dithiothreitol, 100 mM β-mercaptoethanol) were added. This mixture was incubated at 80°C for 1 min, then chilled on ice. After addition of 0.15 mg of Proteinase K, the extract was incubated at 37°C for 1 h. Following the clearing by centrifugation, the supernatant was extracted twice with phenol/chloroform (1 : 1), and once with chloroform/isoamyl (24 : 1). Total RNA was precipitated with isopropanol, resolved in water, then precipitated with 2 M LiCl overnight, and washed with 70% ethanol. Following DNase treatment (DNase I, Roche, Indianapolis, IN, U.S.A.), cDNA was synthesized from 300 ng of RNA using a reverse transcriptase kit (Omniscript, QIAGEN, Valencia, CA, U.S.A.) and 1 U of Taq DNA polymerase (Roche, Indianapolis, IN, U.S.A.). The 3′ region of the *ATS2* gene was amplified for gene expression analysis using the primers 5′-ACGCTAATGGGAACAGGCA-3′ and 5′-AAGATCTCAACATTTAATTCTTC-3′. The coding region of a translation elongation factor EF1α (GenBank Accession no. NM_125432) was used as a control (primers: 5′-ATGCCCCAGGACATCGTGATTTCAT-3′ and 5′-TTGGCGGCACCCTTAGCTGGATCA-3′) (Boisson et al. 2001). Cycle numbers of 28 and 30 were applied for detection of *EF1α* and *ATS2* respectively. The amplified fragments were quantified using Quantity One (BioRad, Hercules, CA, U.S.A.). Each *ATS2* signal was normalized to the *EF1α* signal for calculation of relative amounts.

Heterologous complementation

The *ATS2* open reading frame lacking the predicted transit peptide was generated by RT-PCR using the primers 5′-GAGGATCCAGTGAAAAATTTATGGGCGA-3′ and 5′-CAGGTACCTTAGAGATCCATTGATTCTGC-3′. The open reading frame was fused by blunt end ligation to the *lacZ* gene under the control of an IPTG-inducible promoter in the predigested plasmid pPCR-script AMP SK(+) (Stratagene, La Jolla, CA, U.S.A.) giving rise to plasmid pATS2-s. The plasmid pATS2-s was used to complement the temperature-sensitive phenotype of *E. coli* JC201 ((Coleman 1990); genotype: *plsC thr-1 ara-Δ (gal-attλ)-99 hisG4 rpsL136 xyl-5 mtl-1 lacY1 tsx-78 eda-50 rfbD1 thi-1*). This strain is unable to grow at 42°C due to the deficiency in lysophosphatidic acid acyltransferase encoded in the wild type by *plsC*, but can grow at 30°C. The control strain JC200 was isogenic to JC201 with exception of the *plsC* wild-type allele in JC200.

Microscopy

For the GFP fusion protein localization study, leaf samples of transgenic lines were directly examined using a Meridian Instruments Insight confocal laser scanning microscope (Okemos, MI, U.S.A.). Excitation light was provided by an argon laser at 488 nm. GFP fluorescence was observed with a band-pass filter of 520–560 nm and chlorophyll fluorescence with a 670 nm cut-off filter.

Siliques of different developmental stages from heterozygous *ATS2/ats2* plants were dissected with hypodermic needles. Ovules from individual siliques were mounted on microscope slides in a clearing solution (chloral hydrate, water, glycerol, 8 : 2 : 1 v/v) and cleared for 1 h at 4°C before microscopy. The ovule was observed with a Leica DMLB microscope (Leica Microsystems, Wetzlar, Germany).

Acknowledgments

We thank Hongbo Gao for his help with fluorescence microscopy. We would like to thank Dr. David S. Stephens for the *E. coli* strains JC201 and JC200. This work was supported in parts, by grants from the US Department of Energy Bioscience Program and the MSU Center for Novel Plant Products.

References

Alonso, J.M., Stepanova, A.N., Leisse, T.J., Kim, C.J., Chen, H., Shinn, P., Stevenson, D.K., Zimmerman, J., Barajas, P., Cheuk, R., Gadrinab, C., Heller, C., Jeske, A., Koesema, E., Meyers, C.C., Parker, H., Prednis, L., Ansari, Y., Choy, N., Deen, H., Geralt, M., Hazari, N., Hom, E., Karnes, M., Mulholland, C., Ndubaku, R., Schmidt, I., Guzman, P., Aguilar-Henonin, L., Schmid, M., Weigel, D., Carter, D.E., Marchand, T., Risseeuw, E., Brogden, D., Zeko, A., Crosby, W.L., Berry, C.C. and Ecker, J.R. (2003) Genome-wide insertional mutagenesis of *Arabidopsis thaliana*. *Science* 301: 653–657.

Altschul, S.F., Madden, T.L., Schaffer, A.A., Zhang, J., Zhang, Z., Miller, W. and Lipman, D.J. (1997) Gapped BLAST and PSI-BLAST: a new generation of protein database search programs. *Nucleic Acids Res.* 25: 3389–3402.

Athenstaedt, K. and Daum, G. (1999) Phosphatidic acid, a key intermediate in lipid metabolism. *Eur. J. Biochem.* 266: 1–16.

Arabidopsis Genome Initiative, The (2001) Analysis of the genome sequence of the flowering plant *Arabidopsis thaliana*. *Nature* 408: 796–815.

Babiychuk, E., Müller, F., Eubel, H., Braun, H.P., Frentzen, M. and Kushnir, S. (2003) Arabidopsis phosphatidylglycerophosphate synthase 1 is essential for chloroplast differentiation, but is dispensable for mitochondrial function. *Plant J.* 33: 899–909.

Bechtold, N. and Pelletier, G. (1998) In plant *Agrobacterium*-mediated transformation of adult *Arabidopsis thaliana* plants by vacuum infiltration. *In* Arabidopsis Protocols. Edited by Martinez-Zapater, J. and Salinas, J. pp. 259–266. Humana Press, Totowa, NJ.

Beisson, F., Koo, A.J., Ruuska, S., Schwender, J., Pollard, M., Thelen, J.J., Paddock, T., Salas, J.J., Savage, L., Milcamps, A., Mhaske, V.B., Cho, Y. and Ohlrogge, J.B. (2003) Arabidopsis genes involved in acyl lipid metabolism. A 2003 census of the candidates, a study of the distribution of expressed sequence tags in organs, and a web-based database. *Plant Physiol.* 132: 681–697.

Bhella, R.S. and Mackenzie, S.L. (1994) Nucleotide sequence of a cDNA from *Carthamus tinctorius* encoding a glycerol-3-phosphate acyltransferase. *Plant Physiol.* 106: 1713–1714.

Boisson, M., Gomord, V., Audran, C., Berger, N., Dubreucq, B., Granier, F., Lerouge, P., Faye, L., Caboche, M. and Lepiniec, L. (2001) Arabidopsis glucosidase I mutants reveal a critical role of N-glycan trimming in seed development. *EMBO J.* 20: 1010–1019.

Bourgis, F., Kader, J.C., Barret, P., Renard, M., Robinson, D., Robinson, C., Delseny, M. and Roscoe, T.J. (1999) A plastidial lysophosphatidic acid acyltransferase from oilseed rape. *Plant Physiol.* 120: 913–921.

Brown, A.P., Brough, C.L., Kroon, J.T.M. and Slabas, A.R. (1995) Identification of a cDNA that encodes a 1-acyl-sn-glycerol-3-phosphate acyltransferase from *Limnanthes douglasii*. *Plant Mol. Biol.* 29: 267–278.

Brown, A.P., Coleman, J., Tommey, A.M., Watson, M.D. and Slabas, A.R. (1994) Isolation and characterization of a maize cDNA that complements a 1-acyl sn-glycerol-3-phosphate acyltransferase mutant of *Escherichia coli* and encodes a protein which has similarities to other acyltransferases. *Plant Mol. Biol.* 26: 211–223.

Coleman, J. (1990) Characterization of *Escherichia coli* cells deficient in 1-acyl-sn-glycerol-3-phosphate acyltransferase activity. *J. Biol. Chem.* 265: 17215–17221.

Coleman, J. (1992) Characterization of the *Escherichia coli* gene for 1-acyl-sn-glycerol-3-phosphate acyltransferase (plsC). *Mol. Gen. Genet.* 232: 295–303.

Davies, H.M., Hawkins, D.J. and Nelsen, J.S. (1995) Lysophosphatidic acid acyltransferase from immature coconut endosperm having medium-chain length substrate-specificity. *Phytochemistry* 39: 989–996.

Eberhardt, C., Gray, P.W. and Tjoelker, L.W. (1997) Human lysophosphatidic acid acyltransferase – cDNA cloning, expression, and localization to chromosome 9q34.3. *J. Biol. Chem.* 272: 20299–20305.

Emanuelsson, O., Nielsen, H. and von Heijne, G. (1999) ChloroP, a neural network-based method for predicting chloroplast transit peptides and their cleavage sites. *Protein Sci.* 8: 978–984.

Estelle, M.A. and Somerville, C. (1987) Auxin-resistant mutants of *Arabidopsis thaliana* with an altered morphology. *Mol. Gen. Genet.* 206: 200–206.

Ferro, M., Salvi, D., Brugiere, S., Miras, S., Kowalski, S., Louwagie, M., Garin, J., Joyard, J. and Rolland, N. (2003) Proteomics of the chloroplast envelope membranes from *Arabidopsis thaliana*. *Mol. Cell. Prot.* 2: 325–345.

Ferro, M., Salvi, D., Riviere-Rolland, H., Vermat, T., Seigneurin-Berny, D., Grunwald, D., Garin, J., Joyard, J. and Rolland, N. (2002) Integral membrane proteins of the chloroplast envelope: Identification and subcellular localization of new transporters. *Proc. Natl Acad. Sci. USA* 99: 11487–11492.

Hagio, M., Sakurai, I., Sato, S., Kato, T., Tabata, S. and Wada, H. (2002) Phosphatidylglycerol is essential for the development of thylakoid membranes in *Arabidopsis thaliana*. *Plant Cell Physiol.* 43: 1456–1464.

Hanke, C., Wolter, F.P., Coleman, J., Peterek, G. and Frentzen, M. (1995) A plant acyltransferase involved in triacylglycerol biosynthesis complements an *Escherichia coli* sn-1-acylglycerol-3-phosphate acyltransferase mutant. *Eur. J. Biochem.* 232: 806–810.

Ishizaki-Nishizawa, O., Azuma, M., Ohtani, T., Murata, N. and Toguri, T. (1995) Nucleotide sequence of cDNA from *Spinacia oleracea* encoding plastid glycerol-3-phosphate acyltransferase. *Plant Physiol.* 108: 1342.

Ishizaki, O., Nishida, I., Agata, K., Eguchi, G. and Murata, N. (1988) Cloning and nucleotide sequence of cDNA for the plastid glycerol-3-phosphate acyltransferase from squash. *FEBS Lett.* 238: 424–430.

Knutzon, D.S., Nelsen, J.S., Lardizabal, K.D., Bleibaum, J.L., Hawkins, D.J., Davies, H.M. and Metz, J.G. (1995) Purification and molecular cloning of a medium chain-preferring lysophosphatidic acid acyltransferase from immature coconut endosperm. *Plant Physiol.* 108: 50.

Kunst, L., Browse, J. and Somerville, C. (1988) Altered regulation of lipid biosynthesis in a mutant *Arabidopsis* deficient in chloroplast glycerol-3-phosphate acyltransferase activity. *Proc. Natl Acad. Sci. USA* 85: 4143–4147.

Lassner, M.W., Levering, C.K., Davies, H.M. and Knutzon, D.S. (1995) Lysophosphatidic acid acyltransferase from meadowfoam mediates insertion of erucic-acid at the sn-2 position of triacylglycerol in transgenic rapeseed oil. *Plant Physiol.* 109: 1389–1394.

Logemann, J., Schell, J. and Willmitzer, L. (1987) Improved method for the isolation of RNA from plant tissues. *Anal. Biochem.* 163: 16–20.

Mansfield, S.G., Briarty, L.G. and Erni, S. (1991) Early embryogenesis in *Arabidopsis thaliana*. I. The mature embryo sac. *Can. J. Bot.* 447–460.

Meijer, H.J. and Munnik, T. (2003) Phospholipid-based signaling in plants. *Annu. Rev. Plant Biol.* 54: 265–306.

Murashige, T. and Skoog, F. (1962) A revised medium for rapid growth and bio assays with tobacco tissue cultures. *Physiol. Plant* 15: 473–497.

Nagiec, M.M., Wells, G.B., Lester, R.L. and Dickson, R.C. (1993) A suppressor gene that enables *Saccharomyces cerevisiae* to grow without making sphingolipids encodes a protein that resembles an *Escherichia coli* fatty acyltransferase. *J. Biol. Chem.* 268: 22156–22163.

Nishida, I., Tasaka, Y., Shiraishi, H. and Murata, N. (1993) The gene and the RNA for the precursor to the plastid-located glycerol-3-phosphate acyltransferase of *Arabidopsis thaliana*. *Plant Mol. Biol.* 21: 267–277.

Roughan, P.G. and Slack, C.R. (1982) Cellular organization of glycerolipid metabolism. *Annu. Rev. Plant Physiol.* 33: 97–132.

Sonnhammer, E.L., von Heijne, G. and Krogh, A. (1998) A hidden Markov model for predicting transmembrane helices in protein sequences. *Proc. Int. Conf. Intell. Syst. Mol. Biol.* 6: 175–182.

Thompson, J.D., Higgins, D.G. and Gibson, T.J. (1994) CLUSTAL W: improving the sensitivity of progressive multiple sequence alignment through sequence weighting, position-specific gap penalties and weight matrix choice. *Nucleic Acids Res.* 22: 4673–4680.

Weber, S., Wolter, F.P., Buck, F., Frentzen, M. and Heinz, E. (1991) Purification and cDNA sequencing of an oleate-selctive acyl-ACP: sn-glycerol-3-phosphate acyltransferase from pea chloroplasts. *Plant Mol. Biol.* 17: 1067–1076.

West, J., Tompkins, C.K., Balantac, N., Nudelman, E., Meengs, B., White, T., Bursten, S., Coleman, J., Kumar, A., Singer, J.W. and Leung, D.W. (1997) Cloning and expression of two human lysophosphatidic acid acyltransferase cDNAs that enhance cytokine-induced signaling responses in cells. *DNA Cell Biol.* 16: 691–701.

Yokoi, S., Higashi, S., Kishitani, S., Murata, N. and Toriyama, K. (1998) Introduction of the cDNA for Arabidopsis glycerol-3-phosphate acyltransferase (GPAT) confers unsaturation of fatty acids and chilling tolerance of photosynthesis on rice. *Mol. Breeding* 4: 269–275.

(Received January 31, 2004; Accepted February 23, 2004)